

Quantifying river form variations in the Mississippi Basin using remotely sensed imagery

Z. F. Miller¹, T.M. Pavelsky¹, and G.H. Allen¹

[1]{Department of Geological Sciences, University of North Carolina, Chapel Hill, NC}

Correspondence to: T M. Pavelsky (pavelsky@unc.edu)

Abstract

Geographic variations in river form are often estimated using the framework of downstream hydraulic geometry (DHG), which links spatial changes in discharge to channel width, depth, and velocity through power-law models. These empirical relationships are developed from limited *in situ* data and do not capture the full variability in channel form. Here, we present a dataset of 1.2×10^6 river widths in the Mississippi Basin measured from the Landsat-derived National Land Cover Dataset that characterizes width variability observationally. We construct DHG for the Mississippi drainage by linking DEM-estimated discharge values to each width measurement. Well-developed DHG exists over the entire Mississippi basin, though individual sub-basins vary substantially from existing width-discharge scaling. Comparison of depth predictions from traditional depth-discharge relationships with a new model incorporating width into the DHG framework shows that including width improves depth estimates by, on average, 24%. Results suggest that channel geometry derived from remotely sensed imagery better characterizes variability in river form than do estimates based on DHG.

1 Introduction

River systems connect the terrestrial and oceanic reservoirs of the hydrologic cycle and play a crucial role in landscape development and freshwater resources. Because spatial changes in river form are physical expressions of interaction between a river's flow and the surrounding environment, they are critical to a wide range of scientific and engineering fields. For example, channel geometry, which includes the key variables of width, depth, velocity, slope, and planform shape, reflects local and regional uplift in bedrock and alluvial rivers and

responds to changes in bedrock lithology [Bjerklie, 2007; Whipple, 2004; Montgomery, 2004; Harbor, 1998; Amos and Burbank, 2007; Montgomery and Gran, 2001; Garrett, 1986]. River width and depth play a vital role in CO₂ and nutrient exchange [Butman and Raymond, 2011; Alexander et al, 2000; Wollheim et al., 2006; Peterson et al., 2001]. Aquatic habitat distribution is partially dependent on channel geometry, which both influences the spatial extent of habitats and acts as a barrier to terrestrial species migration [Jowett, 1998; Newson and Newson, 2000; Ayres and Clutton-Brock, 1992; Hayes and Sewlal, 2004]. Humans depend on accurate assessments of river form for understanding flooding hazards, transportation planning, and fisheries management [Hobley et al., 2012; Apel et al., 2009; McCartney, 1986; Troitsky, 1994; Prevost et al., 2003]. Channel shape is also a principal parameter in hydrologic and hydrodynamic models [Paiva et al., 2013; Neal et al., 2012; Yamazaki et al., 2011]. Because of their wide-ranging importance to science and engineering, spatial patterns of channel shape have been studied since at least the work of Leonardo Da Vinci in the 16th century (Humphrey and Abbott, 1867; Bellasis, 1913; Shepherd and Ellis, 1997).

The framework of downstream hydraulic geometry (DHG), developed by Leopold and Maddock [1953], relates spatial patterns of river form to variations in constant-frequency discharge throughout a basin. Three fundamental power-law equations relate width (w), depth (d), and velocity (v) to downstream changes in discharge (Q):

$$w = aQ^b \quad (1a)$$

$$d = cQ^f \quad (1b)$$

$$v = kQ^m \quad (1c)$$

where b , f , m , a , c , and k are exponents and coefficients either derived from physical characteristics or, more commonly, calculated empirically. To facilitate comparison of channel shapes over a large geographic extent, the discharge used in DHG is spatially variable and, ideally, of a constant return period. Some subsequent analyses of natural channels have shown consistency in geometric exponents ($b \approx 0.5$, $f \approx 0.4$; $m \approx 0.1$) [Leopold and Maddock, 1953; Leopold and Miller, 1956; Moody and Troutman, 2002; Chaplin, 2005], while others have found variability in exponents related to changes in basin size, tectonic activity, bedrock lithology, channel vegetation, and levels of human influence [Park, 1977; Klein,

1 1981; Osterkamp and Hedman, 1982; Montgomery and Gran, 2001; Montgomery, 2004;
2 Piestch and Nanson, 2011].

3
4 Most prior investigations of geographic variability in equilibrium channel form rely on *in situ*
5 measurements of river geometry, which are usually available only at widely-spaced locations.
6 This methodology faces two fundamental obstacles in characterizing spatial variations in
7 width and depth. First, the time-intensive nature of *in situ* channel measurement limits the
8 number of measurement locations to a maximum of hundreds [Moody and Troutman, 2002]
9 to thousands [Lee and Julien, 2006]. This restricts either the spatial extent of study areas to
10 smaller basins [e.g. Wolman, 1955] or the density of measurements to wide spacing over
11 larger areas [e.g. Moody and Troutman, 2002; Leopold and Maddock, 1953]. Second, *in situ*
12 channel measurements are often acquired at permanent streamflow gauging sites where
13 accuracy of discharge measurements is usually prioritized, potentially biasing site selection
14 towards desired features such as stable, single-channel cross-sections that may not accurately
15 represent the full range of channel characteristics [Rantz, 1982; Ibbitt, 1997]. These factors
16 suggest that traditional investigations of river shape may not always encompass the full range
17 of spatial variability in channel geometry. Despite these limitations of DHG in describing
18 geometric variations over regional and continental scales, it is often used to estimate channel
19 characteristics in studies of landscape evolution [Tucker and Bras, 1998], nutrient flux
20 [Carleton and Mohamoud, 2013], carbon emissions [Butman and Raymond, 2011; Raymond
21 et al, 2013], width and depth distributions [Andreadis et al., 2013] and the movement of
22 materials, energy, and organisms [Sabo and Hagen, 2012].

23
24 Due to the importance of river form and the difficulty of obtaining wide-scale *in situ* channel
25 measurements, remote sensing has increasingly been used to characterize river width, depth,
26 and velocity [e.g. Legleiter, 2012; Fonstad and Marcus, 2005; Pavelsky and Smith, 2009;
27 Mersel et al., 2013]. As the river parameter most readily observable from remotely sensed
28 data, river width has been quantified using a variety of passive and active sensors since the
29 early stages of the Landsat satellite program in the 1970s [Rango and Salomonson, 1974;
30 Watson, 1991; Smith et al., 1996, Allen et al., 2013]. While remote sensing of channel width
31 has generally covered single rivers or limited spatial extents, recognition of the potential for

large-scale width measurement has recently led to regional and global studies [Pavelsky et al., accepted; Yamazaki et al., in review; Andreadis et al., 2013].

The RivWidth software tool allows automated and spatially continuous channel width measurements from remotely sensed imagery or other gridded data sources [Pavelsky and Smith, 2008]. In this study, we use RivWidth and the Landsat-based National Land Cover Dataset (NLCD) to quantify the spatial variability of river width at approximately mean annual discharge in the Mississippi River Basin and its major sub-basins (Figure 1). We then match width measurements with mean annual discharge values estimated from discharge-drainage area relationships to construct DHG relationships for the basin as a whole and for major sub-basins. Finally, we use our measured widths and estimated discharge values along with *in situ* channel width, area, and discharge measurements from U.S. Geological Survey (USGS) streamflow gauging stations to estimate continuous mean channel depths using a multiple linear regression framework. With these high-resolution, spatially extensive datasets we test the large-scale applicability of downstream hydraulic geometry and create a dataset that replaces DHG-based estimates for many applications.

2 Data and Methods

2.1 Calculating river widths

To develop a high-resolution dataset of river widths over a large area it is necessary to automate width measurement. The RivWidth software tool is designed to calculate river widths from a gridded map of inundation extent [Pavelsky and Smith, 2008]. Its functionality allows calculation of river width at each pixel in an automatically-derived river centerline, and it can be used on both single-channel and multichannel river reaches. Previous studies have used inputs from MODIS, Landsat, SPOT-5 satellite images, and the U.S. Geological Survey's National Land Cover Dataset (NLCD) [Pavelsky and Smith, 2008; Smith and Pavelsky, 2008; Allen et al., 2013; Pavelsky et al., In Press]. In this study, we used the open water class in the NLCD as input to calculate river widths for the Mississippi basin. The NLCD, derived from 30 m Landsat imagery, is an integration of land cover extents from early, peak, and late growing seasons [Homer et al., 2001]. Although inundation extents are not explicitly calibrated to any discharge frequency, we hypothesize that they will, on

average, represent mean growing season streamflow. Tests of this hypothesis are described in Sections 2.2 and 3.2. The NLCD classification was selected for this study because it is a well-established product with thoroughly-described methods, and because it covers nearly the entire Mississippi Basin. A small portion of the basin extends outside the coverage of the NLCD into Canada, and this area was not included in our analysis because the techniques used to classify open water would be inconsistent with the rest of the basin. To create as complete and continuous a dataset as possible, bridges, dams and other small gaps in river extent were manually removed. Widths were measured at one pixel intervals (every 30 to ~42 m) for all visible continuous channels as narrow as one pixel (30 m) in width, although not all rivers as narrow as 30 m were measured (see Section 3.1 for details).

To measure river width from remotely sensed imagery, RivWidth: 1) creates a channel mask by removing water bodies not connected to the river channel; 2) determines the distance from each river pixel to the nearest non-river pixel and calculates the derivative of the resulting distance image (Figure 2c, 2d); 3) determines the river centerline based on the derivative map, in which centerline pixels have values close to zero and all other river pixels have values of approximately one; and 4) calculates the flow width along a line segment orthogonal to the direction of flow at each centerline pixel (Figure 2e). Finally, we eliminated measurements for lakes and reservoirs within the channel systems by removing segments where the NLCD open water class included clear tributary streams adjoining rivers. Further descriptions, updates and downloads are available from *Pavelsky and Smith* [2008] and at <http://www.unc.edu/~pavelsky/>.

2.2 Width validation

To assess the accuracy of RivWidth measurements and the appropriateness of the NLCD for describing channel form at mean flows, we compared *in situ* USGS channel data corresponding to long-term mean annual discharges to validate width measurements. Bankfull discharge is often used in fluvial studies because it approximates the dominant channel-forming flow [e.g. Wolman, 1955; Leopold and Miller, 1956; Chaplin, 2005; Pietsch and Nanson, 2011]. Long-term mean annual discharge is also commonly used to study fluvial processes [Leopold and Maddock, 1953; Griffiths, 1980; Molnar and Ramirez, 2002], and comparison of DHG exponents from a range of flow frequencies shows relatively minor

variation [Knighton, 1974; Griffiths, 1980; Ibbitt, 1997]. Repeated width, depth, and velocity measurements from the USGS at gauging stations throughout the Mississippi Basin are available online [waterdata.usgs.gov/NWIS; Juracek and Fitzpatrick, 2009]. Although unpublished, these data have been used in investigations of channel geometry [Bowen and Juracek, 2011; Stover and Montgomery, 2001]. The number of measurements at each gauge location varies from fewer than ten to thousands across a range of flows. We removed gauges with fewer than 10 years of mean discharge data and those with no discharge or channel measurements after 1970. For each gauge, we estimated the width, depth, and velocity corresponding to mean annual discharge by calculating the mean value of all channel measurements acquired within $\pm 10\%$ of long-term mean annual discharge. Measurements that are clearly erroneous, listed as “poor” by the USGS, taken more than 60 m (two NLCD pixels lengths) upstream or downstream from the gauge location, or measured using a crane along a bridge not perpendicular to the river (therefore not representing true channel width) were removed. We then calculated total error in our width measurements by comparing *in situ* gauge width from the 456 stations meeting our criteria against the mean of the five closest RivWidth-derived width measurements.

2.3 Construction of downstream hydraulic geometry

Construction of DHG relationships requires knowledge of downstream changes in discharge (equation 1a-c) [Leopold and Maddock, 1953]. To build DHG relationships continuously downstream, we used upstream drainage area as a proxy for discharge. We calculated drainage area from the 90-m resolution HydroSHEDS digital elevation model [Lehner et al., 2008] and then assigned the nearest drainage area value to each RivWidth pixel using the methodology developed by Allen et al. [2013] (Figure 3). A linear relationship between upstream drainage area and discharge has been commonly assumed in small basins [e.g. Pazzaglia et al., 1998; Montgomery and Gran, 2001], but for larger rivers this relationship may become nonlinear if the basin includes variations in geology, tectonic deformation, climate, or land use [Stall and Fok, 1968; Galster et al., 2006; Tague and Grant, 2004]. To account for these variations, we developed discharge-drainage area relationships for individual subbasins using values of discharge and drainage area for all USGS stations with ≥ 10 years of approved mean annual discharge. Because discharge-drainage area scaling deviates from linearity over large spatial extents in some basins (Figure 4), we calculated

least-squares linear regressions for each hydrologic accounting unit (i.e. subbasin) in the Ohio, Upper Mississippi, and much of the Missouri and Lower Mississippi basins. In accounting units containing RivWidth measurements in the Missouri, 12 in the Lower Mississippi, and the entire Arkansas basin (excluding the White River), lack of gauging stations, substantial precipitation variability, or large-scale water withdrawals precluded gauge-based discharge estimation (Table 1). These subbasins, along with those not containing rivers large enough to be measured by RivWidth, are not considered in the DHG portion of our analysis.

2.4 Depth estimation

We evaluated three methods of calculating spatial depth distributions, each using channel measurements from 358 USGS gauging stations in regions of the Missouri, Upper Mississippi, and Ohio Basins where both RivWidth measurements and DEM-based discharge estimates were available. First, we developed a traditional depth-discharge relationship for the Mississippi using USGS gauge data from within the basin. Second, we estimated depth using the global depth-discharge equation developed by Moody and Troutman [2002]. Finally, we performed a multiple linear regression of log-transformed *in situ* depth against log-transformed *in situ* width and discharge measurements. We then used our measured widths and estimated discharge values to calculate depth at each centerline pixel and evaluated whether including river width as a variable improves depth estimates over depth-discharge methods. We assessed the effectiveness of including the influence of width in depth estimation by calculating the mean percentage error of each depth estimate relative to USGS-measured depth values.. Due to increasing uncertainty in RivWidth measurements and discharge estimations for smaller rivers, we limited this depth validation to rivers wider than 100 m.

3 Results

3.1 Measurement and distribution of river widths

Using the National Land Cover Dataset, we measured 1.194×10^6 individual channel widths representing 42×10^3 km of rivers in the Mississippi basin (Figure 5). Widths ranged from the minimum pixel size of 30 m to 7400 m in the inundated areas of the Upper Mississippi.

Measurement count and length for each of the five sub-regions of the Mississippi are shown in Table 2. Overall distribution of river widths greater than 100 m and less than 1500 m (Figure 6) closely follows a negative power-law distribution

$$n = 2.1 \times 10^9 W^{-1.9}, \quad (2)$$

where n is the number of pixels of a corresponding width and W is the width. Bars for rivers <100 m in width are included in Figure 6 to indicate the distribution of width data analyzed here, but because we do not capture all rivers at these widths our dataset cannot be used to describe the true distribution of rivers <100 m wide. To evaluate the completeness of this dataset and assess its accuracy, we downloaded historical channel measurements from 2,466 USGS streamflow gauges taken at long-term mean annual discharge. Of these, widths are greater than 30 m (the minimum width theoretically measurable) at 854 locations. Figure 7 shows the percentage of gauges measured in 10 m width increments. Almost all (> 99%) gauge locations wider than 90 m are measured, while the most substantial decrease occurs as width falls below 60 m (two NLCD pixels). The two 100 m gauges not captured by RivWidth are in areas with ambiguous river boundaries, in which the NLCD contains adjacent areas of open water and woody wetlands. At widths between 60 and 100 m, unmeasured stations are more common because not all channels in this size range are adequately captured in the NLCD. The rapid reduction in the percentage of gauges measured at less than 60 m is likely related to difficulties in classifying mixed land-water pixels, which often represent the entire river as width decreases below twice the pixel resolution.

We use two separate methods to estimate the actual length of rivers between 50 and 100 m in the Mississippi Basin. First, comparison with USGS gauge data suggests that RivWidth measured ~68% of gauges 50-100 m in width. We use this percentage as a correction factor, dividing the number of 50-100 m river measurements made here by 0.68 to estimate the correct number of measurements (the dashed box in figure 6). Second, we use equation 2 to extrapolate from the distribution of measurements for rivers wider than 100 m to those between 50 and 100 m in width (the dot in figure 6). These two methods produce nearly identical values.

3.2 Width measurement accuracy

Compared to widths at mean annual discharge from 456 gauging stations in the Ohio/Tennessee, Upper Mississippi, Missouri, and Arkansas regions, mean absolute width error (MAE) is 38 m (Figure 8). Many gauges in the lower Mississippi Region are located in low-lying areas where flow is not confined to a single channel, causing the USGS measurements to include areas that the NLCD classifies as woody wetlands or something other than open water. Because of these complications, gauging stations not on the main stem of the lower Mississippi are excluded. Total mean and median errors of 20 m and 11 m indicate a slight positive bias in RivWidth measurements, although outliers with positive errors of more than 600 m skew the errors substantially. This error can be partitioned into three groups: water mask error, RivWidth error, and inaccuracies in USGS measurements. While stations with measured $W > 60$ m show a median positive bias of only 16 m, stations where $W < 60$ m have a median positive bias of 30 m. This pattern is expected given that small rivers often approach the narrowest width discernable at 30-m spatial resolution. Classification of mixed pixels along banks imparts a theoretical minimum uncertainty of $\frac{1}{2}$ the pixel resolution for each bank crossing (i.e. a minimum of 30 m for single-channel rivers at 30 m resolution; Pavelsky and Smith, 2008).

Inaccuracies associated with the measurement mechanics of RivWidth arise primarily from orthogonal angle errors. Uncertainty results from the predefined spacing of centerline segment endpoints used to define orthogonals to each centerline pixel. In highly sinuous channels where centerlines change direction rapidly, width measurements can be artificially high when orthogonals are not truly perpendicular to the channel. Basin-wide error analysis of widths calculated with endpoint spacings ranging from 7 to 21 pixels showed that inaccuracies are minimized when 11-pixel centerline segments are used, as we do here. In future studies, it may be possible to reduce this source of error by fitting a cubic spline to the channel centerline pixels as described by Legleiter and Kyriakidis (2006). Finally, although we did not attempt to quantify it here due to the large number of stations used, error associated with USGS measurements is minimized through standardized data collection methods [Buchanan and Somers, 1969; Rantz, 1982] and the careful selection of stations as described in section 2.3.

3.3 Estimation of discharge

Using the methods described in section 2.3, we estimated discharge from 0.857×10^6 measurements for rivers totaling 28×10^3 km in length and draining 2.2×10^6 km² of the Mississippi Basin. To assess discharge estimate accuracy, we compared mean discharges from 346 gauging stations in the measured drainage area to the mean of the nearest 5 discharge estimates. Figure 9 shows the nearly 1:1 relationships between estimated discharge and gauge-measured discharge for major sub-basins and for the entire Mississippi. Because ordinary least-squares linear regressions are greatly influenced by high-discharge outliers, we use the Theil-Sen median estimator [Sen, 1968] to derive robust linear regressions for each sub-basin (Table 3). We use the non-parametric Spearman's ρ to characterize goodness-of-fit, as discharges are not normally distributed. Regression slopes close to one and strong correlation between predicted and measured values indicate that estimates of discharge are likely accurate.

3.4 Mississippi Basin downstream hydraulic geometry

Using spatially continuous discharge estimates, we construct width-discharge relationships for the Mississippi Basin and, separately, three of its major sub-basins (Figure 10a-d). Measured widths correspond to discharges ranging from 2.6 m³/s to 19 200 m³/s and drainage areas from 169 km² to 2 940 000 km². Linear least-squares regression of log-transformed width and discharge shows that their relationship can be described by the power-law equation:

$$w = 16.0Q^{0.43} \quad (r^2 = 0.62) \quad (3)$$

However, these values include 38 654 width measurements corresponding to discharge values less than 10 m³/s, which are lower than would be expected for rivers greater than 30 m based on width-discharge relationships from Moody and Troutman (2002) and Leopold and Maddock (1953). 89 % (34 573) of these low-discharge measurements are found in the Missouri sub-basin, where braided streams with high width-depth ratios are common. Of 38 USGS gauging stations with mean discharge < 10 m³/s, width is overestimated in all with a mean bias of 52 m (Fig. 8). As such, it is likely that basin-wide widths for discharges below 10 m³/s result from the inability to resolve multiple channels at the 30 m resolution of the NLCD. If we remove these anomalous measurements, the width DHG equation becomes:

$$w = 13.4Q^{0.46} \quad (r^2 = 0.64) \quad (4)$$

These values of a and b fall close to the range of values calculated for world rivers by Moody and Troutman (2002). However, individual sub-basins show substantial variation from these values, with exponents ranging from 0.3 in the Missouri to 0.63 for the Upper Mississippi (Figure 10). With the exception of the Missouri, variations in discharge account for > 50% of width variability ($r^2 = 0.67$ and 0.73 for the Upper Mississippi and Ohio), indicating that in those sub-basins changes in discharge are the primary control on downstream variations in width. The case of the Missouri Basin will be discussed in more detail in Section 4.

3.5 Estimating depth

Using channel measurements from gauges located on streams measured by RivWidth with corresponding discharge estimates, we compared methods of estimating depth with and without width data. The first method is a simple least-squares linear regression of log-transformed depth and discharge from the gauge station dataset, which results in the power-law expression

$$d = 0.18Q^{0.47} \quad (r^2=0.73) \quad (5)$$

The second method is a multiple linear regression of log-transformed depth against log-transformed discharge and width, which yielded the equation

$$\ln(d)=0.44-0.82\ln(w)+0.83 \ln(Q) \quad (r^2=0.85) \quad (6)$$

Figure 11 shows depths calculated from equation 6 for the Ohio, Upper Mississippi, Missouri, and main stem of the Lower Mississippi using our estimated discharge and measured widths.

Basin-wide mean depth error is 40% for the two DHG estimations, and 31% for the multiple regression method (Table 4). Figures 12a-b compare the percentage error of equation (6) to that of the two simple downstream hydraulic geometry relationships (Equation 5 and Moody and Troutman [2002]). Although mean relative error is nearly identical in the Ohio and Upper Mississippi sub-basins, the two discharge-based methods both substantially overestimate depth for seven gauging stations along the Platte River in the Missouri sub-basin, leading to relative errors of 50%. The disparity between approaches in the Missouri accounts for the higher error of the discharge-based equations in the basin as a whole.

4 Discussion and Conclusions

In this study, we present one of the first high-resolution, spatially continuous width datasets covering a major river basin. The utility of remote-sensing based measurement of channel geometry is increasingly recognized for both characterizing width-discharge relationships and applications for hydrologic modeling [Andreadis et al., 2013; Pavelsky et al., accepted; Yamazaki et al., in review]. Construction of a width frequency distribution using 1.2×10^6 measurements (Equation 2) shows that Mississippi widths follow a power-law distribution ($n = 2.1 \times 10^9 W^{-1.9}$) comparable to that found by Pavelsky et al. [accepted] for the 8.5×10^5 km² Yukon basin ($n = 1.78 \times 10^9 W^{-1.72}$). Similarities between these two basins—which represent highly contrasting geology, ecology, climate, and flow regimes—suggest that width distributions in other basins may follow similar patterns.

Basin-wide width-discharge relationships are characteristic of the downstream hydraulic geometry framework proposed by Leopold and Maddock [1953]. However, in the global analysis of Moody and Troutman [2002], changes in discharge account for >94% of width variation compared to 62% for the Mississippi basin in this study. While error inherent in the RivWidth dataset undoubtedly accounts for some of the higher width variability observed here, it seems unlikely that channel width corresponds as precisely to discharge as is shown in previous work. One explanation for this discrepancy is the widely-spaced and non-random site selection for *in situ* channel measurements. To facilitate accurate discharge measurements, USGS gauging station selection criteria suggest using straight channel segments located away from tributary junctions, with only one channel and easy access (Rantz, 1982). It is not unreasonable to assume that similar site selection bias exists for most *in situ* channel and discharge measurement locations. In particular, the measurement bias towards single-channel rivers in previous DHG studies using gauge data may explain the higher width variability observed in this dataset. Finally, previous investigations of DHG have used datasets incorporating a much wider range of discharges [e.g. Moody and Troutman, 2002] than the rivers used in this study, which may result in higher r^2 values for those width-discharge relationships. Conversely, the fact that our dataset does not include smaller streams may result in a less well-defined best-fit regression.

Individual sub-basins demonstrate different levels of adherence to traditional downstream hydraulic geometry. Missouri sub-basin channel widths increase with discharge at a much lower rate ($b=0.3$) than has been found in previous studies (e.g. Leopold and Maddock, 1953; Moody and Troutman, 2002) with a much lower proportion of width variation explained by discharge increases ($r^2=0.44$). Conversely, the Ohio sub-basin closely matches previous findings ($b=0.48$; $r^2=0.72$). Several factors could explain this discrepancy. Multi-channel rivers are much more common in the Missouri sub-basin than in the Ohio; despite similar total measured lengths (Table 2) the Missouri contains nearly 2.5 times as many multi-channel measurements as the Ohio. While multiple channel crossings increase inherent RivWidth measurement error as explained in section 3.2, braided streams are also likely to show increased width variability in response to changes in climate and flow regime [Schumm, 2005]. The Missouri sub-basin also has some of the highest levels of human influence and control in North America, factors that can affect variability in channel form. In particular, dam construction has varied but pronounced effects on channel morphology [Gregory, 2006; Williams and Wolman, 2004]. Williams [1978] documented highly variable channel narrowing on the Platte River as it crosses the Great Plains due to upstream flow regulation. Human impacts on stream form and flow across the central section of the Missouri drainage may lead to the high width variability and lower than expected increase in width with discharge observed in the Missouri sub-basin. In addition, the substantially drier climate and greater topographic relief in the upstream portions of the Missouri, relative to the Ohio or Upper Mississippi, may also influence the variations in DHG observed here by affecting the balance of water and sediment supplies in the different subbasins.

Human influence also likely plays a role in the high b -value (0.64) observed in the Upper Mississippi sub-basin. In larger rivers—particularly along the main stem of the Mississippi—lock and dam control structures artificially widen the channel or connect it to secondary channels in its floodplain. Because of difficulties in differentiating the main stem of the Mississippi from ancillary channels and inundated floodplains that connect to the main channels in the NLCD, these features are included in the width-discharge dataset. While the high b -value may not represent the natural width changes, we believe it accurately describes present-day inundation extent along the Upper Mississippi more effectively than would a lower width exponent.

1
2 In sub-basins with well-developed width-discharge relationships, traditional depth-discharge
3 DHG predicts depth well without inclusion of additional information on river width. In the
4 Ohio and Upper Mississippi sub-basins, depth estimates based on the two d - Q relationships
5 show similar accuracy to that of the multiple regression estimation that incorporates width
6 (Equation 6). In the Missouri sub-basin, however, both traditional DHG methods
7 substantially overestimate depth for wide, shallow rivers compared to the multiple regression
8 analysis. Although basin-wide absolute error is not significantly reduced, consistent
9 overestimation of depth for wide, shallow rivers like the Platte suggests that in applications
10 where depths are based on downstream hydraulic geometry [e.g. Alexander, 2000], factoring
11 width into depth estimations substantially reduces uncertainty. This improvement results from
12 the underlying assumption of continuity in the relationship between depth, discharge, width,
13 and velocity; measuring width while assuming locally constant flow eliminates one degree of
14 freedom from the depth equation.

15
16 Several potential sources of error must be addressed when studying channel form using
17 remotely sensed data. The largest sources of uncertainty in our Mississippi dataset are
18 inherent to the input imagery. Because higher pixel resolution decreases classification error,
19 increases total channel length, and decreases the size of smallest rivers measured, selecting
20 appropriate input data is critical. Figure 7 indicates that all rivers greater than three times the
21 pixel resolution and substantial numbers of smaller rivers are measured. While our results
22 suggest that the NLCD represents an approximation of river extent close to mean discharge,
23 there are clear instances where channels are wider than expected due to connectivity with the
24 surrounding floodplain, misclassification of channel boundary pixels, or potential use of
25 images taken during times of higher than mean flows. To reduce the error associated with the
26 input water mask, future investigations should use a consistent and effective river
27 classification scheme on images taken during periods of the desired flow state. Finally,
28 RivWidth must be configured properly, as the segment length used to calculate the orthogonal
29 direction can create non-perpendicular cross-sections when poorly chosen. Other methods of
30 calculating orthogonals to the river centerline, especially implementation of algorithms
31 described by Legleiter and Kyriakidis (2006), may help to minimize this source of error in
32 future studies.

1
2 Provided these sources of error are addressed, RivWidth offers the capability to measure river
3 width at a high resolution over large basins with small and predictable error. Despite the
4 importance of river form and flow, *in situ* river monitoring capabilities have declined over the
5 last several decades [Vorosmarty et al., 2001], highlighting the importance of remote sensing
6 techniques that can produce high-resolution, spatially continuous observations of river
7 channels over large areas [Alsdorf et al., 2007]. Although significant challenges remain in
8 using remotely sensed channel observations to produce discharge measurements, non-real
9 time estimations of river flow relying on width measurement have been made [LeFavour and
10 Alsdorf, 2004; Smith and Pavelsky, 2008]. In addition, multivariate equations for prediction
11 of streamflow [e.g. Bjerklie et al., 2003] often combine river width measurements with
12 information on slope and other river form data. As the most widely observable of the three
13 primary dimensions of river discharge, understanding variations in width is a critical first step
14 in characterizing discharge from remotely sensed data. Because RivWidth produces maps of
15 river centerline it may be useful in characterizing the planform shape of rivers (e.g. via indices
16 of sinuosity and braiding), which would help to reveal downstream patterns in river form.
17 Additionally, intersection of river centerlines with a high-resolution DEM would allow
18 estimation of mean slope, another key variable in understanding river form (Bjerklie 2007).

19
20 In addition to its importance in the measurement of discharge, remote sensing of river width
21 contributes to the accuracy of hydrologic and hydraulic modeling. While width parameters
22 are often characterized through empirically derived discharge relationships [e.g. Yamazaki et
23 al., 2011, Andreadis et al., 2013], the utility of widths from satellite imagery in improving
24 hydraulic modeling of river and floodplain dynamics is increasingly recognized [Neal et al.,
25 2012; Schumann et al., 2009]. Given growing interest in river modeling at continental and
26 global scales and the importance of rivers in natural and human systems, this paper and other
27 recent studies [e.g. Yamazaki et al., in review] demonstrate how data from future satellite
28 missions such as the Surface Water and Ocean Topography mission (jointly under
29 development by the United States and France) can measure the spatial and temporal
30 variability in Earth's surface water resources [Fu et al., 2012]. These products, combined
31 with ongoing work to produce Landsat-derived width datasets globally, will allow for more

accurate characterization of spatial variability in channel form than is currently afforded by empirically-derived estimation methods

ACKNOWLEDGEMENTS

This study was funded by NASA New Investigator Grant #NNX12AQ77G, managed by Ming-Ying Wei. We thank Benjamin Mirus for his thoughtful comments on a draft of the manuscript. We also thank Carl Legleiter, Mark Fonstad, and one anonymous reviewer for their useful suggestions.

REFERENCES

- Alexander, R. B., Smith, R. A., and Schwarz, G. E.: Effect of stream channel size on the delivery of nitrogen to the Gulf of Mexico, *Nature*, 403(6771), 758-761, 2000.
- Allen, G. H., Barnes, J. B., Pavelsky, T. M., and Kirby, E.: Lithologic and tectonic controls on bedrock channel form at the northwest Himalayan front, *J. Geophys. Res. Earth Surf.*, 118, 1806-1825, doi:10.1002/jgrf.20113, 2013
- Alsdorf, D. E., Rodríguez, E., and Lettenmaier, D.P.: Measuring surface water from space, *Rev. Geophys.*, 45, RG2002, doi:10.1029/2006RG000197, 2007.
- Amos, C. B., and Burbank, D. W.: Channel width response to differential uplift, *J. Geophys. Res.*, 112, F02010, doi:10.1029/2006JF000672, 2007.
- Andreadis, K. M., Schumann, G. J-P., and Pavelsky, T. M.: A simple global river bankfull width and depth database, *Water Resour. Res.*, 49(10), 7164-168, doi: 10.1002/wrcr.20440, 2013.
- Apel, H., Aronica, G. T., Kreibich, H., and Thieken, A. H.: Flood risk analyses—how detailed do we need to be?, *Natural Hazards*, 49(1), 79-98, doi: 10.1007/s11069-008-9277-8, 2009.
- Ayres, J. M., and Clutton-Brock, T. H.: River boundaries and species range size in Amazonian primates. *The American Naturalist*, 140(3), 531-537, 1992.
- Bellasis, E. S.: River and canal engineering: the characteristics of open flowing streams, and the principles and methods to be followed in dealing with them, E. & F. N. Spon, Limited, London, 1913.

1 Bjerklie, D.M.: Estimating the bankfull velocity and discharge for rivers using remotely
2 sensed river morphology information, *J. Hydrol.*, 341, 144-155, 2007.

3 Bowen, M. W., and Juracek, K. E.: Assessment of the Geomorphic Effects of Large Floods
4 Using Streamgage Data: the 1951 Floods in Eastern Kansas, USA, *Physical*
5 *Geography*, 32(1), 52-77, 2011

6 Buchanan, T. J., and Somers, W. P.: Discharge measurements at gaging stations, U.S. Geol.
7 Surv. Tech. Water Resour. Invest, Book 3, Chap. A8, United States Government Printing
8 Office, Washington 1969.

9 Butman, D., and Raymond, P. A.: Significant efflux of carbon dioxide from streams and
10 rivers in the United States. *Nature Geoscience*, 4(12), 839-842, doi:10.1038/NGEO1294,
11 2011.

12 Carleton, J. N., and Mohamoud, Y. M.: Effect of Flow Depth and Velocity on Nitrate Loss
13 Rates in Natural Channels¹, *Journal of the American Water Resources Association*, 49(1),
14 205-216, doi:10.1111/jawr.12007, 2013.

15 Chaplin, J. J.: Development of regional curves relating to bankfull-channel geometry and
16 discharge to drainage area for streams in Pennsylvania and selected areas of Maryland, U.S.
17 Geol. Surv. Scientific Investigations Report 2005-5147, 40pp, 2005.

18 Fonstad, M. A., and Marcus, W. A.: Remote sensing of stream depths with hydraulically
19 assisted bathymetry (HAB) models, *Geomorphology*, 72(1), 320-339,
20 doi:10.1016/j.geomorph.2005.06.005, 2005.

21 Fu, L. L., Alsdorf, D., Morrow, R., Rodriguez, E., and Mognard, N. (Eds.): SWOT: The
22 Surface Water and Ocean Topography Mission: Wide-Swath Altimetric Measurement of
23 Water Elevation on Earth, JPL-Publication 12-05, 228 pp. Jet Propul. Lab., Pasadena, Calif.,
24 2012.

25 Galster, J. C., Pazzaglia, F. J., Hargreaves, B. R., Morris, D. P., Peters, S. C., and Weisman,
26 R.N.: Effects of urbanization on watershed hydrology: The scaling of discharge with drainage
27 area, *Geology*, 34(9), 713-716, doi: 10.1130/G22633.1, 2006.

28 Garrett, W.P.: River meanders and channel size, *J. Hydrol.*, 88, 147-164.

29 Gregory, K. J.: The human role in changing river channels, *Geomorphology*, 79(3), 172-191,
30 doi:10.1016/j.geomorph.2006.06.018, 2006.

1 Griffiths, G. A.: Hydraulic geometry relationships of some New Zealand gravel bed
2 rivers. *Journal of Hydrology (NZ)*, 19, 106-118, 1980.

3 Harbor, D. J.: Dynamic equilibrium between an active uplift and the Sevier River, Utah, *The*
4 *Journal of Geology*, 106(2), 181-194, 1998.

5 Hayes, F. E., and Sewlal, J.A.N.: The Amazon River as a dispersal barrier to passerine birds:
6 effects of river width, habitat and taxonomy, *J Biogeography*, 31(11), 1809-1818, 2004.

7 Hobley, D. E., Sinclair, H. D., and Mudd, S. M.: Reconstruction of a major storm event from
8 its geomorphic signature: The Ladakh floods, 6 August 2010, *Geology*, 40(6), 483-486, doi:
9 10.1130/G32935.1, 2012.

10 Homer, C., Huang, C., Yang, L., Wylie, B., and Coan, M.: Development of a 2001 national
11 land cover database for the United States, *Photogramm. Eng. Remote Sens.*, 70, 829-840,
12 2004.

13 Humphreys, C. A., and Abbot, L.H.: Report upon the physics and hydraulics of the
14 Mississippi River, US Government Printing Office, Washington, DC, 1867.

15 Ibbitt, R. P.: Evaluation of optimal channel network and river basin heterogeneity concepts
16 using measured flow and channel properties, *J. Hydrology*, 196(1-4), 119-138, 1997.

17 Jowett, I. G.: Hydraulic geometry of New Zealand rivers and its use as a preliminary method
18 of habitat assessment, *Regulated Rivers: Research & Management*, 14(5), 451-466, 1998.

19 Juracek, K. E., and Fitzpatrick, F. A.: Geomorphic applications of stream-gage
20 information, *River Research and Applications*, 25(3), 329-347, 2009.

21 Klein, M.: Drainage area and the variation of channel geometry downstream, *Earth Surf.*
22 *Process. Landforms*, 6(6), 589-593, 1981.

23 Knighton, A. D.: Variation in width-discharge relation and some implications for hydraulic
24 geometry, *Geological Society of America Bulletin*, 85(7), 1069-1076, 1974.

25 Lee, J. S., and Julien, P. Y.: Downstream hydraulic geometry of alluvial channels, *J. Hyd.*
26 *Eng.*, 132(12), 1347-1352, 2006.

27 LeFavour, G., and Alsdorf, D.: Water slope and discharge in the Amazon River estimated
28 using the shuttle radar topography mission digital elevation model, *Geophys. Res. Lett.*, 32,
29 L17404, doi:10.1029/2005GL023836, 2005.

1 Legleiter, C. J.: Mapping river depth from publicly available aerial images, *River Research*
2 *and Applications*, 29(6), 760-780, doi:10.1002/rra.2560, 2012.

3 Legleiter, C.J., and Kyriakidis, P.C.: Forward and inverse transformations between Cartesian
4 and channel-fitted coordinate systems for meandering rivers, *Mathematical Geology*, 38(8),
5 9270958, doi:10.1007/s11004-006-9056-6, 2006.

6 Lehner, B., Verdin, K., and Jarvis, A.: New Global Hydrography Derived From Spaceborne
7 Elevation Data, *Eos Trans. AGU*, 89(10), 93-94, doi: 10.1029/2008eo100001, 2008.

8 Leopold, L.B. and Maddock, T.: The hydraulic geometry of stream channels and some
9 physiographic implications, U.S. Geol. Surv. Prof. Paper, 252, United States Government
10 Printing Office, Washington, 1953.

11 Leopold, L.B. and Miller, J. P.: Ephemeral streams—hydraulic factors and their relation to the
12 drainage net, U.S. Geol. Surv. Prof. Paper 282-a, United States Government Printing Office,
13 Washington, 1956.

14 McCartney, B.: Inland Waterway Navigation Project Design, *J. Waterway, Port, Coastal,*
15 *Ocean Eng.*, 112(6), 645–657, 1986.

16 Mersel, M. K., Smith, L. C., Andreadis, K. M., and Durand, M. T.: Estimation of river depth
17 from remotely sensed hydraulic relationships, *Water Resour. Res.*, 49, 3165–3179,
18 doi:10.1002/wrcr.20176, 2013.

19 Molnar, P., and Ramirez, J. A.: On downstream hydraulic geometry and optimal energy
20 expenditure: case study of the Ashley and Taieri Rivers. *J. Hydrology*, 259(1), 105-115,
21 2002.

22 Montgomery, D. R. and Gran, K. B.: Downstream variations in the width of bedrock
23 channels, *Water Resour. Res.*, 37, 1841-1846, doi:10.1029/2000WR900393, 2001.

24 Montgomery, D.R.: Observations on the role of lithology in strath terrace formation and
25 bedrock channel width, *American Journal of Science*, 304, 454-476, 2004.

26 Moody, J. A., and Troutman, B. M.: Characterization of the spatial variability of channel
27 morphology, *Earth Surf. Proc. Land.*, 27(12), 1251-1266, doi:10.1002/esp.403, 2002.

28 Neal, J., Schumann, G., and Bates, P.: A subgrid channel model for simulating river
29 hydraulics and floodplain inundation over large and data sparse areas, *Water Resour. Res.*, 48,
30 W11506, doi:10.1029/2012WR012514, 2012.

1 Newson, M. D., and Newson, C. L.: Geomorphology, ecology and river channel habitat:
2 mesoscale approaches to basin-scale challenges, *Progress in Physical Geography*, 24(2), 195-
3 217, 2000.

4 Osterkamp, W.R., Hedman, E.R.: Perennial streamflow characteristics related to channel
5 geometry and sediment in the Missouri River Basin, USGS Professional Paper, 1242, 1982.

6 Paiva, R. C. D., Buarque, D. C., Collischonn, W., Bonnet, M.-P., Frappart, F., Calmant, S.,
7 and Mendes, C. A. B.: Large- scale hydrologic and hydrodynamic modeling of the Amazon
8 River basin, *Water Resour. Res.*, 49, 1226–1243, doi:10.1002/wrcr.20067, 2013.

9 Park, C. C.: World-wide variations in hydraulic geometry exponents of stream channels: an
10 analysis and some observations, *J. Hydrology*, 33(1), 133-146, 1977.

11 Pavelsky, T.M. and Smith, L.C.: RivWidth: A software tool for the calculation of river widths
12 from remotely sensed imagery, *IEEE Geoscience and Remote Sensing Letters*, 5(1), 70-73,
13 2008.

14 Pavelsky, T.M. and Smith, L.C.: Remote sensing of suspended sediment concentration, flow
15 velocity, and lake recharge in the Peace-Athabasca Delta, Canada, *Water Resour. Res.*, 45,
16 W11417, doi:10.1029/2008WR007424, 2009.

17 Pavelsky, T.M., Allen, G. H., and Miller, Z. F.: Remote Sensing of river widths in the Yukon
18 River Basin, In: *Remote Sensing of the Terrestrial Water Cycle*, Geophysical Monograph
19 206, Lakshmi, V. [Ed], 131-141, American Geophysical Union, Washington, 2015.

20 Pazzaglia, F.J., Gardner, T.W., and Merritts, D.J.: Bedrock fluvial incision and longitudinal
21 profile development over geologic time scales determined by fluvial terraces, in: *Rivers over
22 rock: Fluvial processes in bedrock channels*, American Geophysical Union Geophysical
23 Monograph 107, Tinkler, K.J. and Wohl, E. E. [Eds], 207–236, American Geophysical Union,
24 Washington, 1998.

25 Peters, B.J., Wollheim, W. M., Mulholland, P. J., Webster, J. R., Meyer, J. L., Tank, J. L.,
26 Marti, E., Bowden, W. B., Valett, H.M., Hershey, A. E., McDowell, W. H., Dodds, W. K.,
27 Hamilton, S. K., Gregory, S., and Morrall, D. D.: Control of nitrogen export from watersheds
28 by headwater streams, *Science*, 292(5514), 86-90, doi: 10.1126/science.1056874, 2001.

29 Pietsch, T. J., and Nanson, G. C.: Bankfull hydraulic geometry; the role of in-channel
30 vegetation and downstream declining discharges in the anabranching and distributary

1 channels of the Gwydir distributive fluvial system, southeastern Australia,
2 Geomorphology, 129(1), 152-165, doi:10.1016/j.geomorph.2011.01.021, 2011.

3 Prevost, E., Parent, E., Crozier, W., Davidson, I., Dumas, J., Gudbergsson, G., Hindar, K.,
4 McGinnity, P., MacLean, J., and Saettemi, L. M.: Setting biological reference points for
5 Atlantic salmon stocks: transfer of information from data-rich to sparse-data situations by
6 Bayesian hierarchical modeling, ICES J. Mar. Sci, 60(6): 1177-1193, doi:
7 10.1016/j.icesjms.2003.08.001, 2003.

8 Rango, A., and Salomonson, V. V.: Regional flood mapping from space, Water Resour.
9 Res., 10, 473-484, doi: 10.1029/WR010i003p00473, 1974.

10 Rantz, S. E.: Measurement and computation of streamflow; Volume 1, measurement of stage
11 and discharge, US Geological Survey Water-Supply Paper, 2175, United States Government
12 Printing Office, Washington, 1982.

13 Raymond, P.A., Hartmann, J., Lauerwald, R., Sobek, S., McDonald, C., Hoover, M., Butman,
14 D., Striegl, R., Mayorga, E., Humborg, C., Kortelainen, P., Durr, H., Meybeck, M., Ciais, P.,
15 and Guth, P.: Global carbon dioxide emissions from inland waters. Nature, 503(7476), 355-
16 359, 2013.

17 Sabo, J. L., and Hagen, E. M.: A network theory for resource exchange between rivers and
18 their watersheds, Water Resour. Res, 48, W0515, doi:10.1029/2011WR010703, 2012.

19 Schumann, G., Bates, P. D., Horritt, M. S., Matgen, P., and Pappenberger, F.: Progress in
20 integration of remote sensing-derived flood extent and stage data and hydraulic models, Rev.
21 Geophys., 47, RG4001, doi:10.1029/2008RG000274, 2009.

22 Schumm, S. A.: River variability and complexity, Cambridge University Press, Cambridge,
23 UK, 2005.

24 Seaber, P. R., Kapinos, F. P., and Knapp, G.L.: Hydrologic unit maps, U.S. Geol. Surv.
25 Water-Supply Paper, 2254, 63 pp, United States Government Printing Office, Washington,
26 1987.

27 Sen, P. K.: Estimates of the regression coefficient based on Kendall's tau, Journal of the
28 American Statistical Association, 63(324), 1379-1389, 1968.

1 Shepherd, R.G., Ellis, B.N: Leonardo da Vinci's Tree and the Law of Channel Widths—
2 Combining Quantitative Geomorphology and Art in Education, *Journal of Geoscience*
3 *Education*, 45, 425-427, 1997.

4 Smith, L.C. and Pavelsky, T. M.: Estimation of river discharge, propagation speed and
5 hydraulic geometry from space: Lena River, Siberia, *Water Resour. Res.*, 44, W03427,
6 doi:10.1029/2007WR006133, 2008.

7 Smith, L. C., Isacks, B. L., Bloom, A. L., and Murray, A. B.: Estimation of discharge from
8 three braided rivers using synthetic aperture radar satellite imagery: Potential application to
9 ungaged basins, *Water Resour. Res.*, 32, 2021-2034, doi:10.1029/96WR00752, 1996.

10 Stall, J.B. and Fok Y.: Hydraulic geometry of Illinois streams, University of Illinois Water
11 Resources Center Research Report no. 15, 52 pp, 1968.

12 Stover, S. C., and Montgomery, D.R.: Channel change and flooding, Skokomish River,
13 Washington, *J. Hydrology*, 243(3), 272-286, 2001.

14 Tague, C., and Grant, G.E.: A geological framework for interpreting the low-flow regimes of
15 Cascade streams, Willamette River Basin, Oregon, *Water Resour. Res.*, 40, W04303,
16 doi:10.1029/2003WR002629, 2004.

17 Troitsky, M. S.: Planning and design of bridges, John Wiley, New York, NY, 1994.

18 Tucker, G. E., and Bras, R. L.: Hillslope processes, drainage density, and landscape
19 morphology, *Water Resour. Res.*, 34, 2751-2764, doi:10.1029/98WR01474, 1998.

20 Vörösmarty, C., Askew, A., Berry, R., Birkett, C., Döll, P., Grabs, W., Hall, A., Jenne, R.,
21 Kitaev, L., Landwehr, J., Keeler, M., Leavesley, G., Schaake, J., Strzepek, K., Sundarvel, S.,
22 Takeuchi, K., and Webster, F.: Global water data: A newly endangered species, *EOS Trans.*
23 *AGU* 82(5), 54-58, 2001.

24 Watson, J. P.: A visual interpretation of a Landsat mosaic of the Okavango Delta and
25 surrounding area. *Remote Sens. Environ.*, 35(1), 1-9, 1991.

26 Whipple, K. X.: Bedrock rivers and the geomorphology of active orogens. *Annu. Rev. Earth*
27 *Planet. Sci.*, 32, 151-185, doi: 10.1146/annurev.earth.32.101802.120356, 2004.

28 Wickham, J. D., Stehman, S. V., Fry, J. A., Smith, J. H., and Homer, C. G.: Thematic
29 accuracy of the NLCD 2001 land cover for the conterminous United States, *Remote Sens.*
30 *Env.*, 114(6), 1286-1296., doi:10.1016/j.rse.2010.01.018, 2010.

- 1 Williams, G. P.: The case of the shrinking channels — the North Platte and Platte Rivers in
2 Nebraska, US Geological Survey Circular 781, United States Government Printing Office,
3 Washington, 1978.
- 4 Williams, G. P., and Wolman, M. G.: Downstream effects of dams on alluvial rivers, U.S.
5 Geol. Surv. Prof. Paper, 1286, 83 pp., United States Government Printing Office,
6 Washington, 1984.
- 7 Wohl, E. E.: Limits of downstream hydraulic geometry, *Geology*, 32(10), 897-900, doi:
8 10.1130/G20738.1, 2004.
- 9 Wollheim, W. M., Vorosmarty, C. J., Peterson, B. J., Seitzinger, S. P., and Hopkinson, C. S.:
10 Relationship between river size and nutrient removal, *Geophys. Res. Lett.*, 33, L06410,
11 doi:10.1029/2006GL025845, 2006.
- 12 Wolman, M. G.: The natural channel of Brandywine Creek, Pennsylvania, U.S. Geol. Surv.
13 Prof. Paper 271, 56 pp., United States Government Printing Office, Washington, 1955.
- 14 Yamazaki, D., Kanae, S., Kim, H., and Oki, T.: A physically based description of floodplain
15 inundation dynamics in a global river routing model, *Water Resour. Res.*, 47, W04501,
16 doi:10.1029/2010WR009726, 2011.
- 17 Yamazaki, D., O'Loughlin, F., Trigg, M. A., Miller, Z. F., Pavelsky, T. M., and Bates, P. D.:
18 Development of the Global Width Database for Large Rivers, *Water Resour. Res.*, 50(4),
19 3467-3480, 2014.

1 Table 1. Portions of the Mississippi Basin included in and excluded from the analysis

	Ohio	Upper Mississippi	Missouri		Arkansas	Lower Mississippi	
Accounting units excluded from DHG estimates	None	None	100200, 100402, 100901, 101301, 101303, 101702, 101900, 102500,	100302, 100500, 100902, 101302, 101600, 101800, 102100, 102802	All basins other than 110100 (Upper White River excluded)	080202, 080302, 080701, 080703, 080802, 080902,	080204, 080403, 080702, 080801, 080901, 080903
Total area included (excluded) in DHG	527900 km ² (0 km ²)	429200 km ² (0 km ²)	727600 km ² (621700 km ²)		57900 km ² (584400 km ²)	119600 km ² (129400 km ²)	

2

3 Table 2. Width measurement count and river length

Hydrologic Region	Ohio- Tennessee	Upper Mississippi	Lower Mississippi	Arkansas- Red	Missouri	Total
n	304685	223259	137055	218604	311029	1194632
Length (km)	10761	7872	4819	7699	10944	42095

4

5 Table 3. Estimated discharge-measured discharge regressions

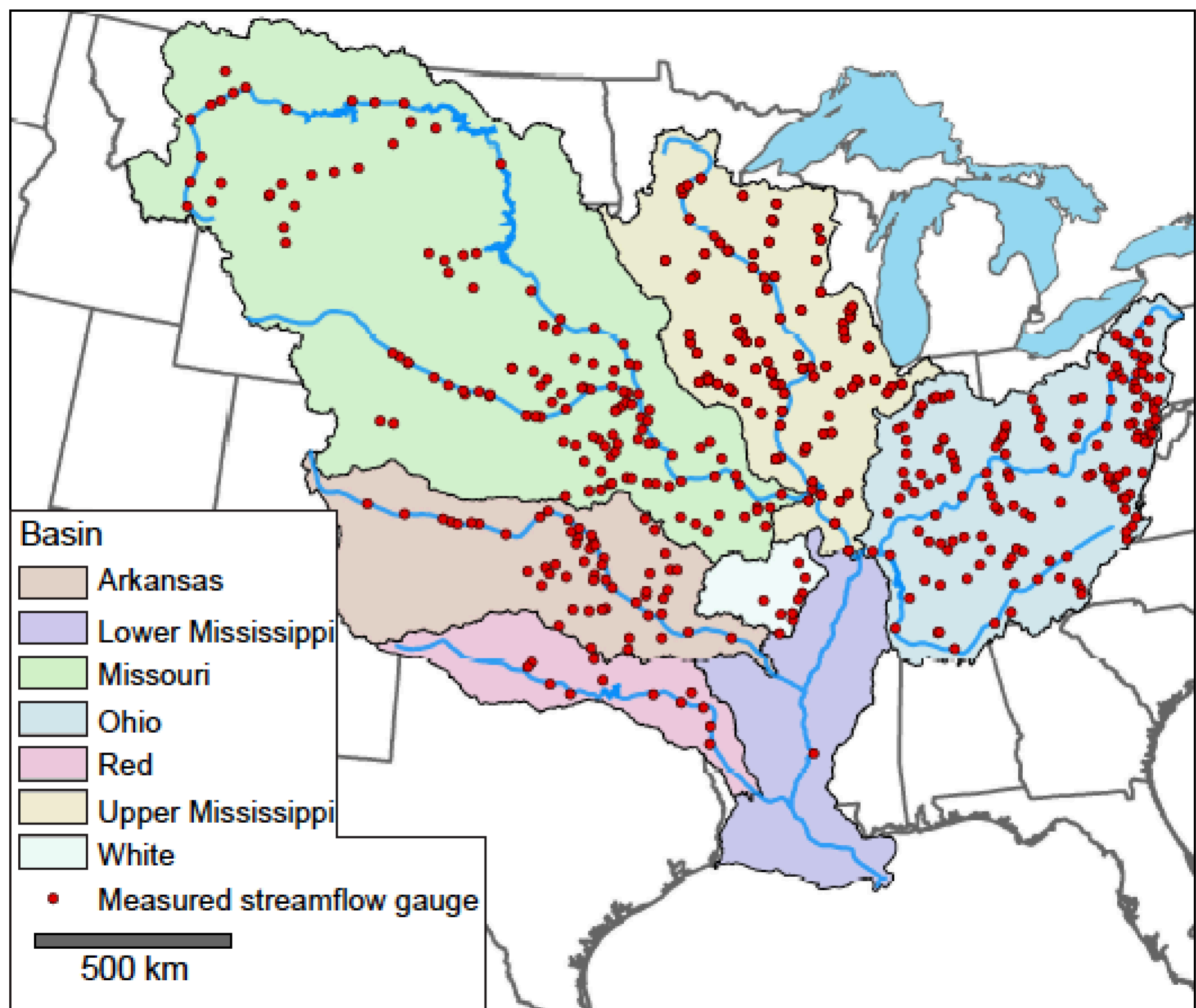
	Ohio	Upper Mississippi/ Lower main stem	Missouri	Total
Regression	y=1.00x-0.59	y=0.98x+1.8	y=0.95x+2.0	y=0.98x+0.8
Spearman's ρ	0.99	0.99	0.99	0.99

6

7 Table 4. Mean absolute depth errors (%)

Sub-basin	Depth Only	Depth and Width	Moody- Troutman
Ohio	34%	35%	37%
Upper Mississippi	40%	33%	35%
Missouri	55%	33%	53%
Total	43%	34%	42%

1 Figures and Captions



2

3 Figure 1. Major sub-basins of the Mississippi and USGS gauging stations used for width validation

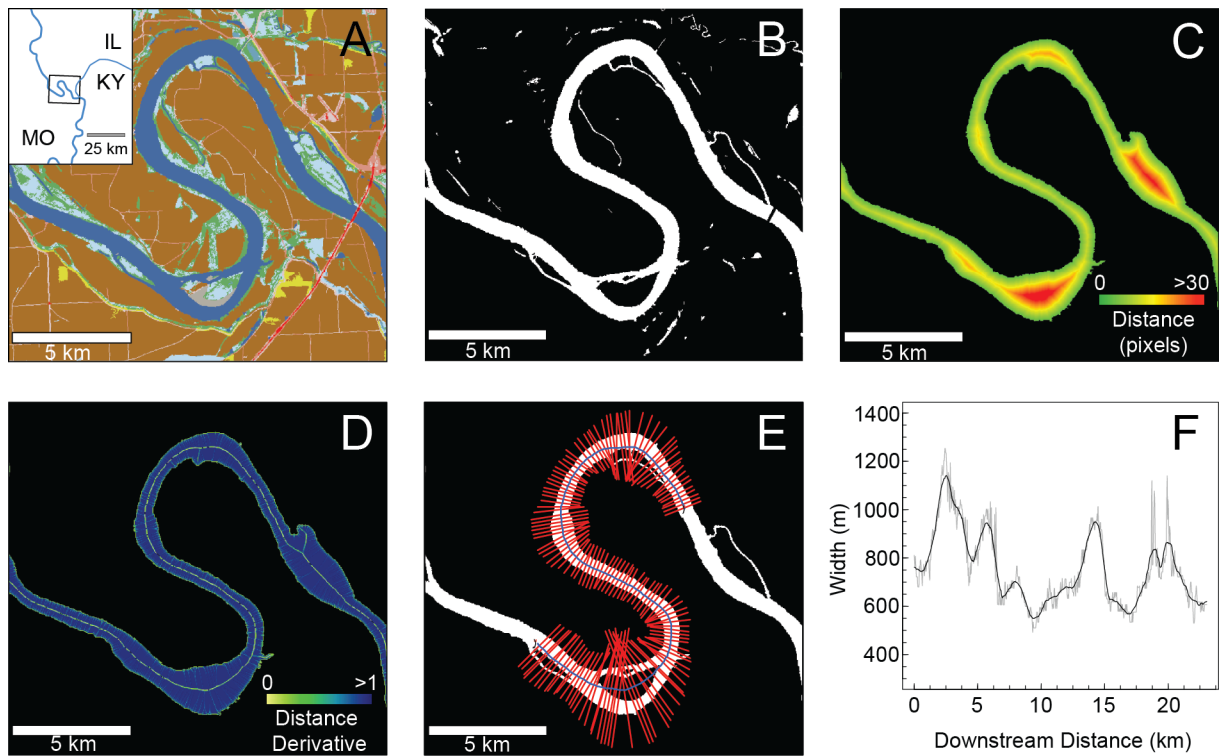
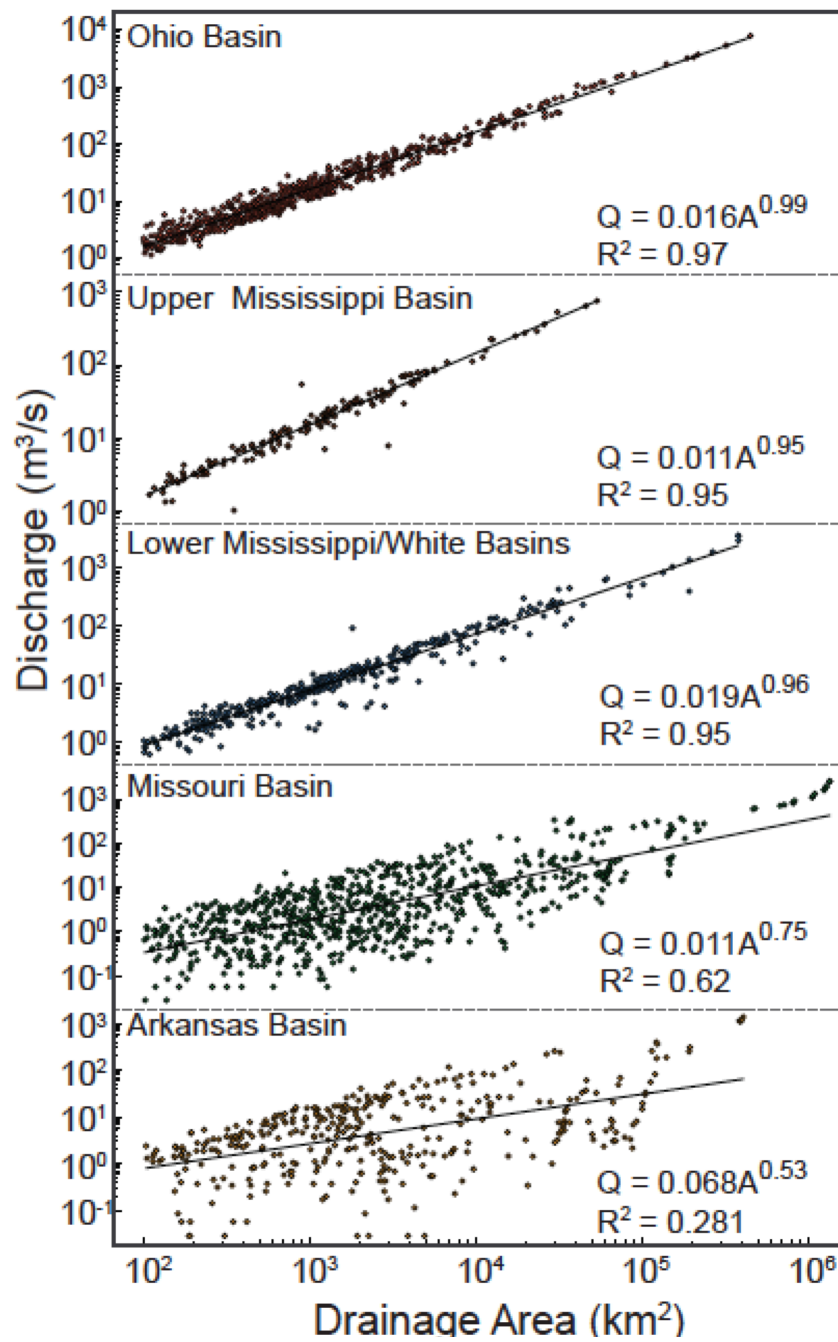
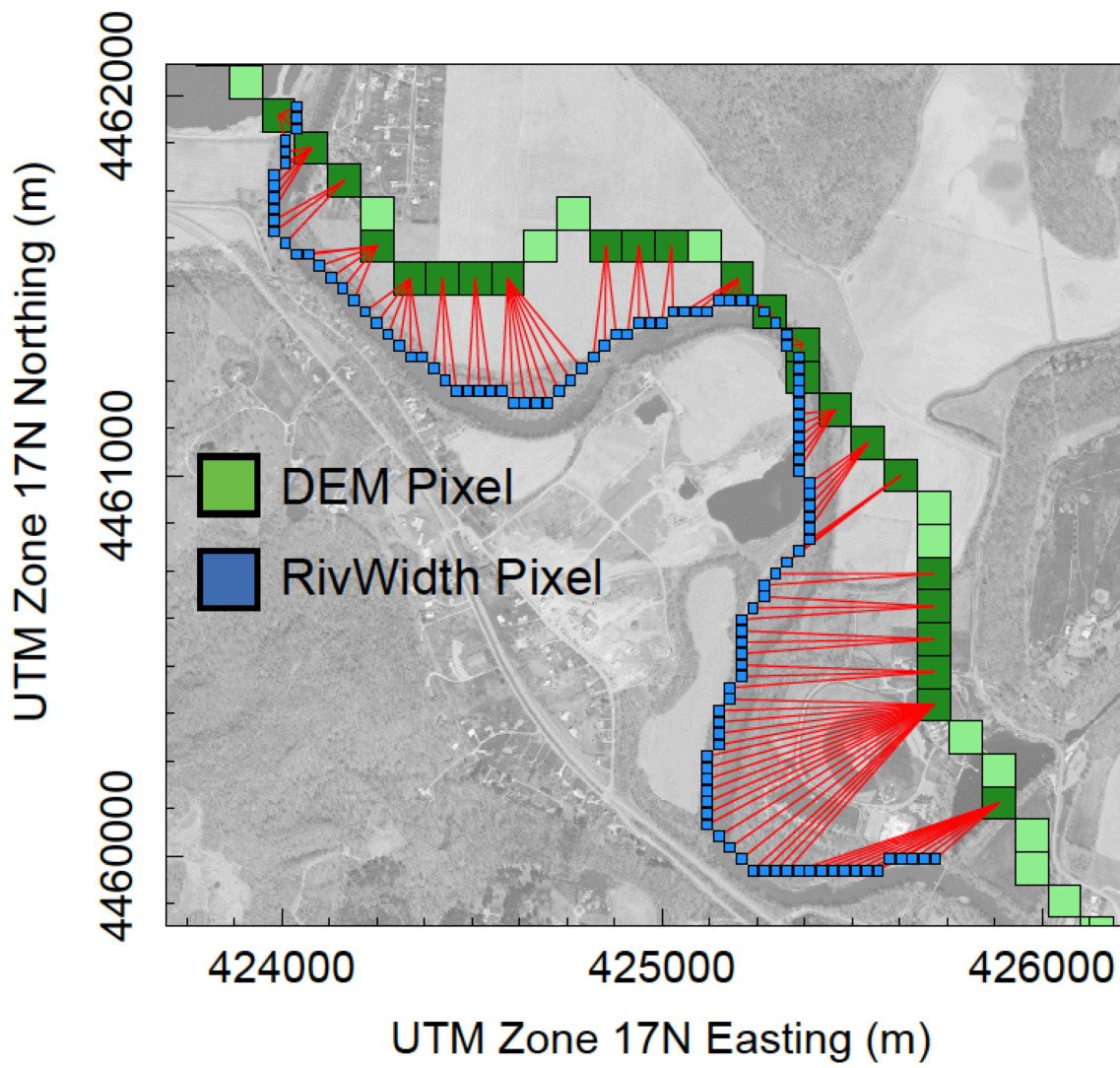


Figure 2. Inputs, intermediate steps, and products for calculation of river width in this study: A) National Land Cover Dataset; B) binary water mask of the open water classification; C) distance image based on a filled channel mask; D) derivative of distance image used to calculate the centerline; E) flow width measurements along orthogonal line segments to each centerline pixel; F) plot of raw (grey) and smoothed (black) continuous widths.



1
2 Figure 3. Linking RivWidth and DEM measurements: RivWidth measurements for the Walhonding River near
3 Coshcocton, PA, matched to the nearest downstream DEM-derived channel pixels with drainage area values.



1
 2 Figure 4. Discharge-drainage area relationships for sub-basins of the Mississippi; exponents close to one indicate
 3 a nearly linear fit in the Ohio, Upper and Lower Mississippi sub-basins, but there is substantial deviation from
 4 unity in the Missouri and Arkansas sub-basins.

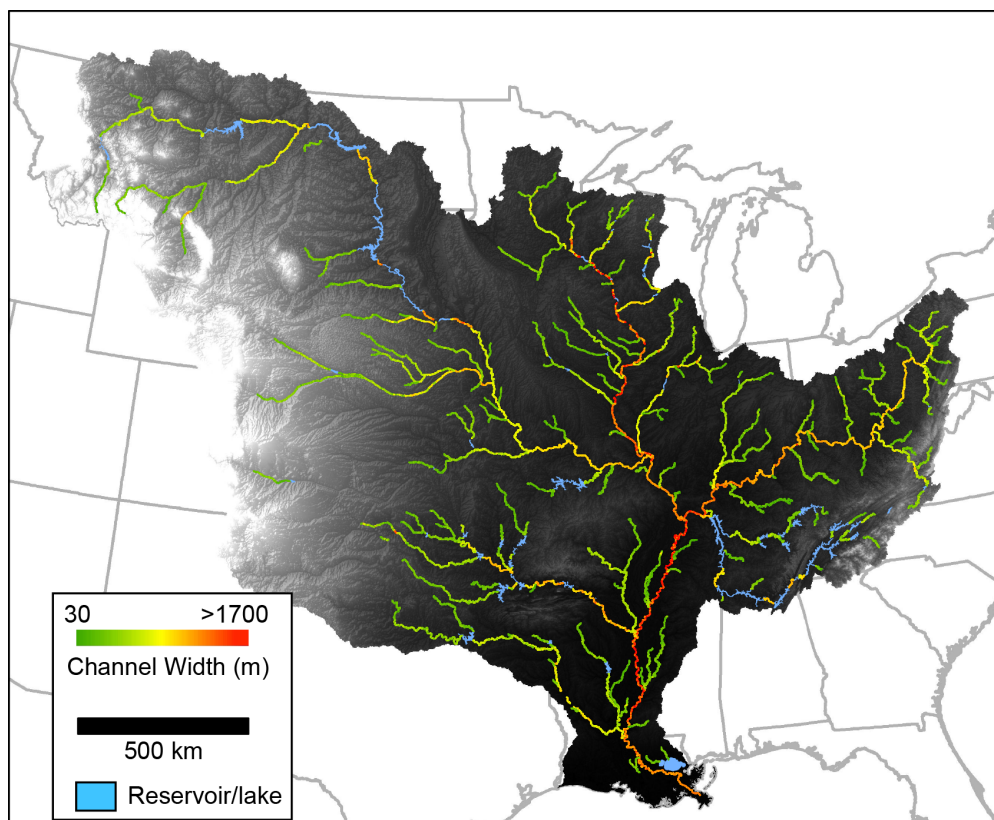


Figure 5. Mississippi River width map (shown with USGS HydroSHEDS DEM) of $\sim 1.2 \times 10^6$ observations at 30 m resolution based on the NLCD open water classification

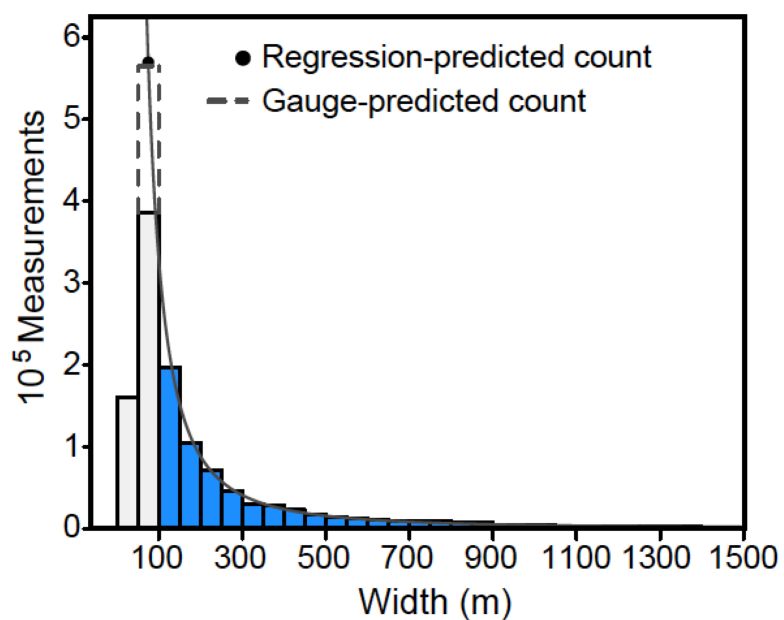
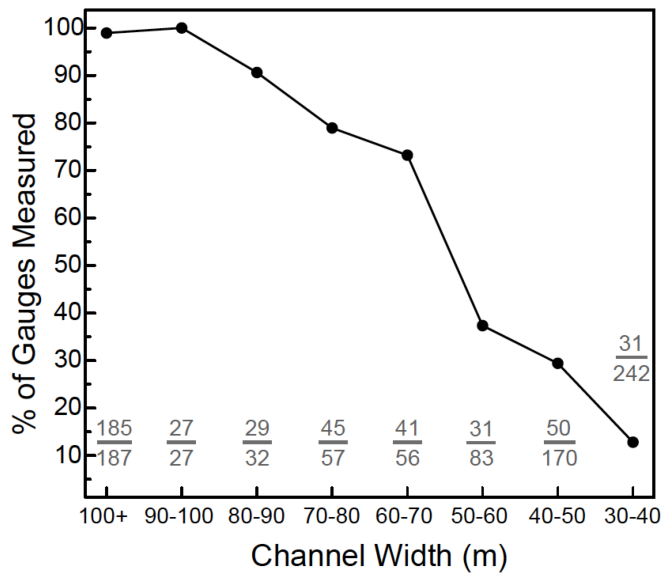
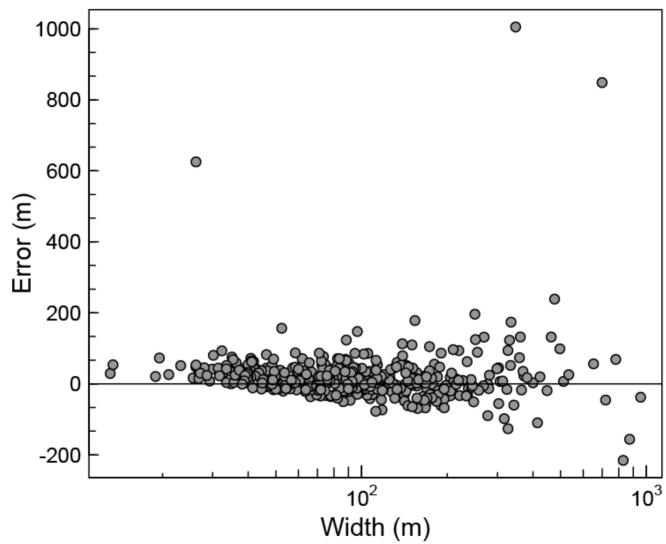


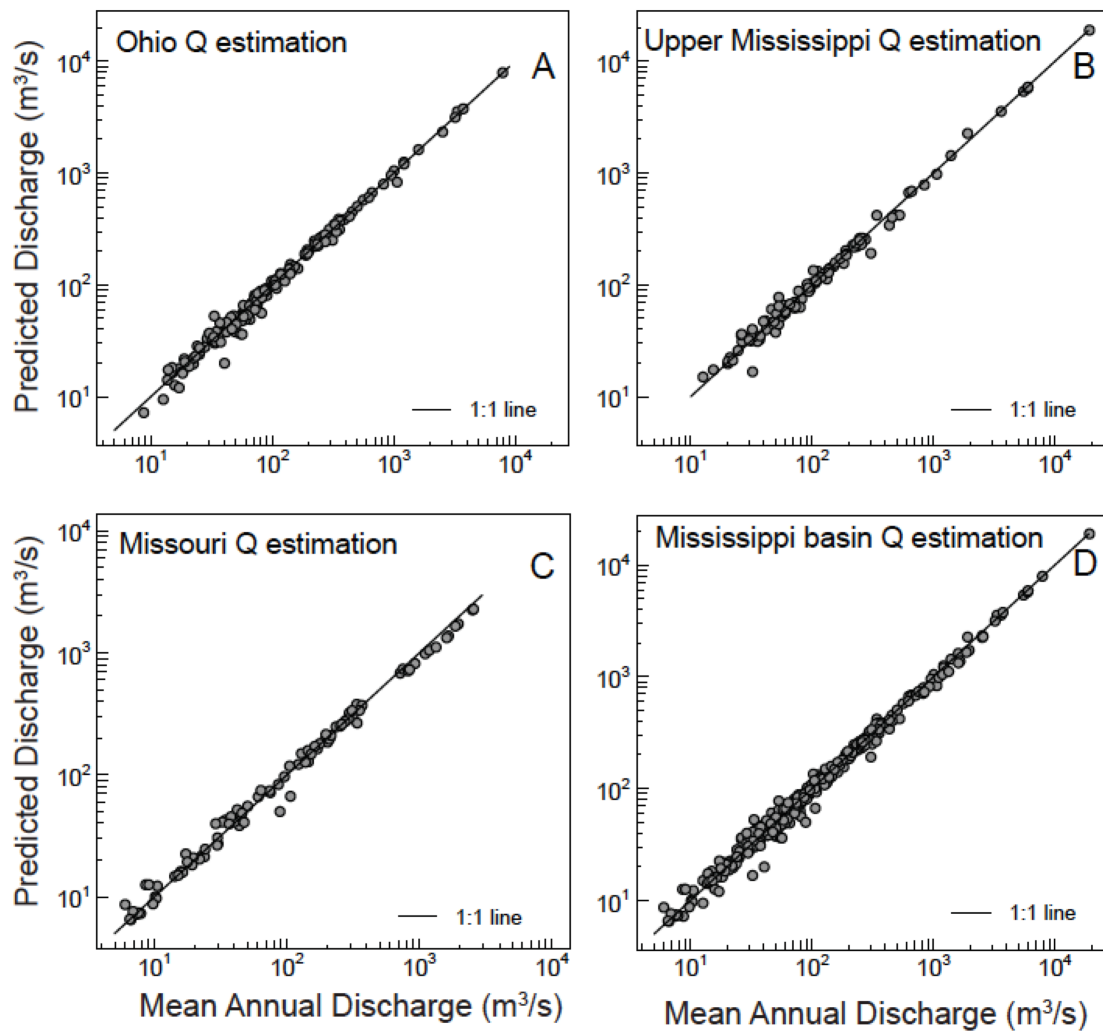
Figure 6. Width distributions for all rivers >100 m (blue bars) and many rivers < 100 m (grey bars); black circle represents measurements predicted by the 100-1500 m distribution regression ($n=570,000$, black line); dashed gray lines show estimated number of 50-100m rivers from the frequency distribution of USGS river gauges ($n=565,000$).



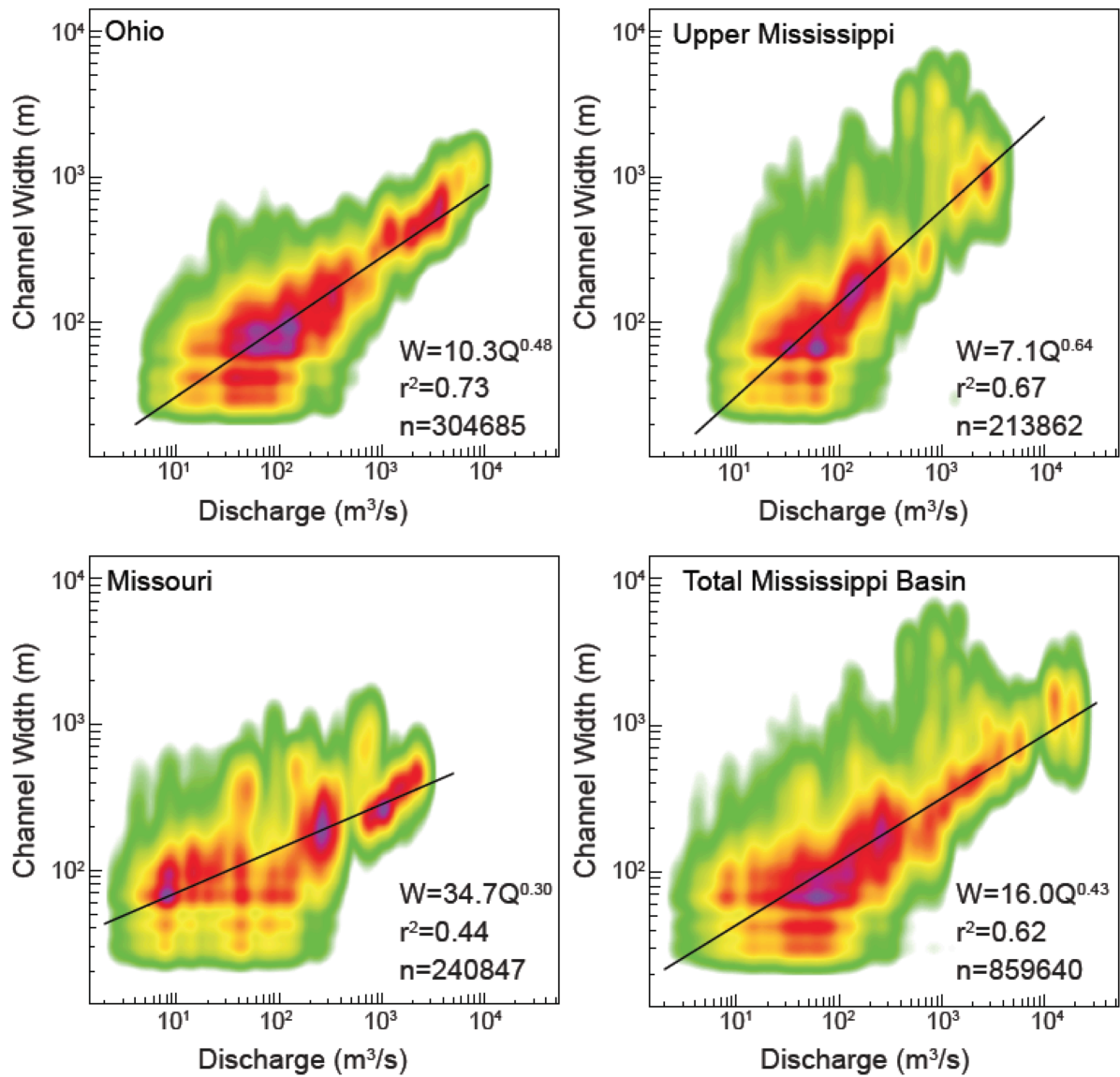
1
2 Figure 7. Percentage of USGS gauging stations measured in this study, binned by *in situ* channel width; grey
3 fractions indicate number measured out of total gauges per 10-m width range.



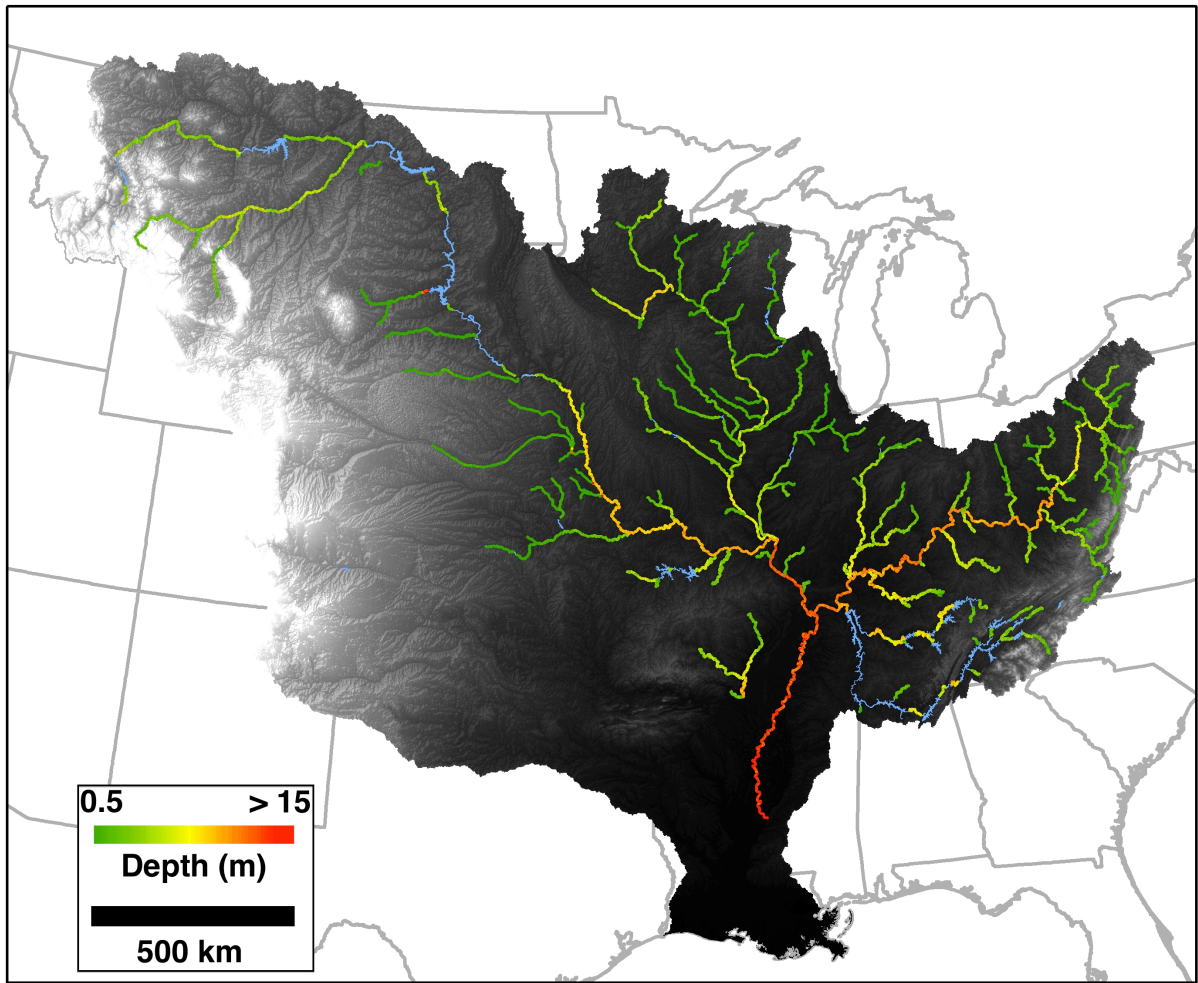
4
5 Figure 8. Width measurement error based on *in situ* channel measurements from 456 USGS streamflow gauging
6 stations



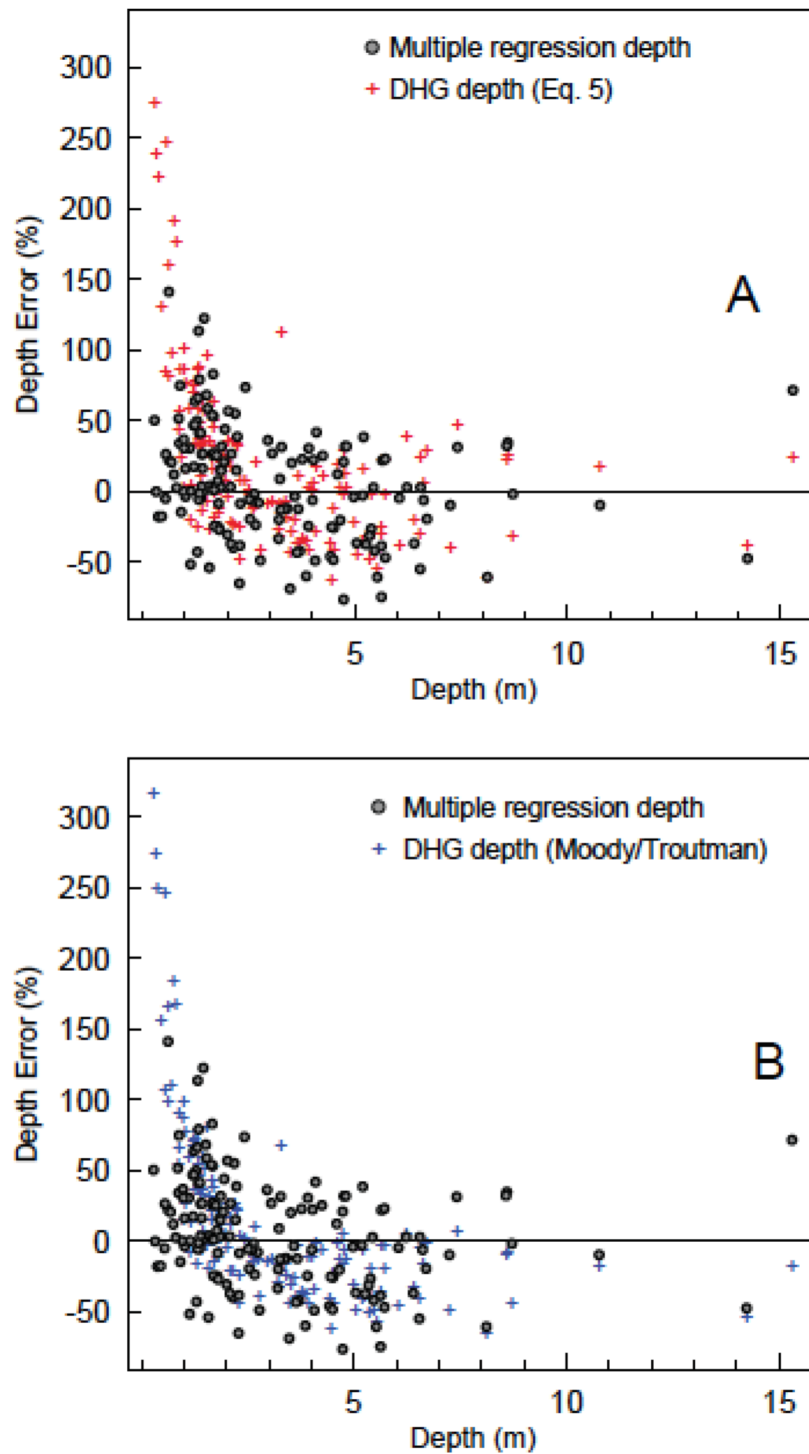
1
2 Figure 9. Estimated and USGS measured mean discharges for 346 gauging stations in the Mississippi basin.



1
2 Figure 10. Density plots of width versus discharge for the Ohio, Upper Mississippi, Missouri, and entire
3 Mississippi basin. Linear fits represent downstream hydraulic geometry relationships analogous to Equation 1a.



- 1
- 2 Figure 11. 8×10^5 mean depths in the Mississippi basin estimated using multiple regression of d against Q and w ;
- 3 lakes shown in blue



1
2 Figure 12. Relative depth error for multiple regression method (circles) and A) DHG estimate (this study); B)
3 DHG estimate (Moody and Troutman, 2002)
4
5